Ophiopogonin B suppresses the metastasis and angiogenesis of A549 cells *in vitro* and *in vivo* by inhibiting the EphA2/Akt signaling pathway

MEIJUAN CHEN[1,2], CHENG HU[1,2], YUANYUAN GUO[1,2], RILEI JIANG[1,2], HUIMIN JIANG[1], YU ZHOU[1], HAIAN FU[3,4], MIANHUA WU[2] and XU ZHANG[1,2]

[1]School of Medicine and Life Sciences and [2]Jiangsu Collaborative Innovation Center of Traditional Chinese Medicine (TCM) Prevention and Treatment of Tumors, Nanjing University of Chinese Medicine, Nanjing 210023, P.R. China; Departments of [3]Pharmacology and [4]Hematology and Medical Oncology, Emory University School of Medicine, Atlanta, GA 30322, USA

Received December 7, 2017; Accepted June 12, 2018

DOI: 10.3892/or.2018.6531

Abstract. Lung adenocarcinoma is the most common metastatic cancer, and is associated with high patient mortality. Therefore, investigation of anti-metastatic treatments for lung adenocarcinoma is crucial. Ophiopogonin B (OP-B) is a bioactive component of Radix Ophiopogon Japonicus, which is often used in Chinese traditional medicine to treat pulmonary disease. Screening of transcriptome and digital gene expression (DGE) profiling data in NSCLC cell lines showed that OP-B regulated the epithelial-mesenchymal transition (EMT) pathway in A549 cells. Further results showed that 10 μmol/l OP-B downregulated EphA2 expression and phosphorylation (Ser897) in A549 cells but upregulated them in NCI-H460 cells. Meanwhile, the Ras/ERK pathway was unaffected in A549 cells and stimulated in NCI-H460 cells. More importantly, detection of the EMT pathway showed that OP-B treatment increased the epithelial markers ZO-1 and E-cadherin and decreased the expression of the mesenchymal marker N-cadherin and the transcriptional repressors Snail, Slug and ZEB1. Furthermore, through Transwell migration and scratch wound healing assays, we found that 10 μmol/l OP-B significantly reduced the invasion and migration of A549 cells. *In vivo*, we found that 75 mg/kg OP-B inhibited A549 cell metastasis in a pulmonary metastasis nude mouse model. In addition, we also found that 10 μmol/l OP-B significantly inhibited tube formation in EA.hy926 cells. The expression of VEGFR2 and Tie-2, the phosphorylation of Akt (S473) and PLC (S1248), and the levels of EphA2 and phosphorylated EphA2 (S897) were all inhibited by OP-B in this cell line. *In vivo*, using a Matrigel plug assay, we found that OP-B inhibited angiogenesis and the hemoglobin content of A549 transplanted tumors. Taken together, OP-B inhibited the metastasis and angiogenesis of A549 cells by inhibiting EphA2/Akt and the corresponding pathway. The investigation gives new recognition to the anticancer mechanism of OP-B in NSCLC and this compound is a promising inhibitor of metastasis and angiogenesis of lung adenocarcinoma cells.

Correspondence to: Dr Mianhua Wu or Dr Xu Zhang, Jiangsu Collaborative Innovation Center of Traditional Chinese Medicine (TCM) Prevention and Treatment of Tumors, Nanjing University of Chinese Medicine, Nanjing, Jiangsu 210023, P.R. China
E-mail: wmh7001@163.com
E-mail: zhangxu@njucm.edu.cn

Key words: Ophiopogonin B, epithelial-mesenchymal transition, metastasis, angiogenesis, adenocarcinoma, EphA2/Akt

Introduction

In the clinic, lung adenocarcinoma has the highest mortality rate of all cancers due to its tendency to metastasize at an early stage (1,2). Preventing metastasis is crucial for improving the survival rate of these patients. During cancer metastasis, angiogenesis and epithelial-mesenchymal transition (EMT) are crucial events (3,4). Eph receptors have been reported to be involved in many biological processes, including angiogenesis and cell migration (5). In gastric cancer cells, EphA2 was reported to promote EMT through the Wnt-β-catenin pathway (6). Recent genome-wide analyses revealed that EphA2 is commonly overexpressed in non-small cell lung cancer (NSCLC), which is correlated with poor prognosis (7-10). Through binding to its ligand ephrinA1, EphA2 phosphorylates multiple tyrosine residues, leading to activation of itself and its downstream molecules. In certain carcinoma cells, Src and focal adhesion kinase (FAK) were reported to be the downstream regulators of the ephrinA1/EphA2 pathway, instructing cells to move and facilitating tissue invasion of ephrin-sensitive carcinomas (11). In addition, through interacting with EGFR and HER2, Src also transduces survival signals to downstream effectors, such as phosphoinositide 3-kinases (PI3Ks), Akt and signal transducer and activator of transcription 3 (STAT3) (12).

Our previous study reported that Ophiopogonin B (OP-B) inhibited the PI3K/Akt pathway in the NCI-H157, NCI-H460

and A549 cell lines. However, the sensitivity of these cell lines to OP-B differed greatly (13,14). Whether EphA2 is the key molecular affecting the sensitivity of different cell lines to OP-B is still unknown.

In the present study, we found that OP-B regulated EMT in only A549 cells. Further detection of EphA2 in A549 and NCI-H460 cells showed that OP-B inhibited the phosphorylation of EphA2 in A549 cells but not in NCI-H460 cells.

Further experiments were carried out to verify the effect of OP-B on A549 cell metastasis *in vitro* and *in vivo*; meanwhile, the effects of OP-B on EphA2- and EMT-related molecules such as E-cadherin, ZO-1, N-cadherin, vimentin, Snail, Slug and Zeb1 were also detected to uncover their role in the process of OP-B-regulated metastasis in A549 cells.

The present study may provide useful information for the clinical application of Radix Ophiopogon Japonicus in NSCLC treatment.

Materials and methods

Reagents. Ophiopogonin B (OP-B) (MW: 722.9, HPLC ≥98%) was purchased from Nanjing Zelang Medical Technology Co. (Nanjing, China). The compound was initially dissolved in dimethyl sulfoxide (DMSO) (Sigma-Aldrich; Merck KGaA, Darmstadt, Germany) as a stock solution. For treatment of cells, OP-B was diluted in culture medium to the appropriate concentrations, and the final concentration of DMSO was <0.01%.

The primary antibodies against E-cadherin (cat. no. sc-3195), ZO-1 (cat. no. sc-8193), vimentin (cat. no. sc-5741), N-cadherin (cat. no. sc-13116), Snail (cat. no. sc-3879), Slug (cat. no. sc-9585), TCF8/ZEB1 (cat. no. sc-3396), p-SRC (Tyr416) (cat. no. sc-6943), p-FAK (Tyr397) (cat. no. sc-8556), p-Stat3 (Tyr705) (cat. no. sc-9145), Stat3 (cat. no. sc-12640), p-Stat5 (Tyr694) (cat. no. sc-9351), Stat5 (cat. no. sc-9363), VEGFR2 (cat. no. sc-9698), Tie-2 (cat. no. sc-4224), p-Akt (Ser473) (cat. no. sc-4060), p-PLCγ1 (Ser1248) (cat. no. sc-8713), EphA2 (cat. no. sc-6997) and p-EphA2 (Ser897) (cat. no. sc-6347) were purchased from Cell Signaling Technology (Danvers, USA). The secondary antibody was also from Cell Signaling Technology.

Cell culture. The NSCLC cell lines A549, NCI-H460 and NCI-H596 were obtained from the Institute of Biochemistry and Cell Biology (Shanghai, China). Cells were grown in Gibco® RPMI-1640 medium (Thermo Fisher Scientific, Inc., Waltham, MA, USA) supplemented with 10% fetal bovine serum (FBS) and 100 U/ml penicillin-streptomycin mixed antibiotics and were cultured under 5% CO_2 at 37˚C. Total RNA was immediately extracted from the cell lines treated with or without OP-B for 2 h.

Digital gene expression (DGE) library preparation and sequencing. Total RNA was extracted using the Illumina Gene Expression Sample Prep Kit (Illumina, Inc., San Diego, CA, USA) according to the manufacturer's protocol. Quality and quantity analyses of total RNA, DGE library preparation, and sequencing were carried out at Huada Genomics Co., Ltd. (Shenzhen, China). We used a false discovery rate (FDR) ≤0.05 and the absolute value of log2 ratio ≥1 as the thresholds to judge the significance of gene expression differences (15).

Western blot analysis. After being treated with different concentrations of OP-B, the cells were lysed in RIPA buffer. The protein concentrations of the supernatants were determined by the BCA protein assay. Equal amounts of protein (50 μg) were loaded onto gels, separated by 12% SDS-PAGE and then transferred onto nitrocellulose membranes (Millipore, Billerica, MA, USA). The membranes were incubated with appropriate primary antibodies (1:1,000) at 4˚C overnight, followed by a 1-h incubation with HRP-conjugated secondary antibodies (anti-rabbit or anti-mouse immunoglobulin G, 1:2,000) at room temperature. Then, the protein level was quantified by enhanced chemiluminescence (ECL; Bio-Rad Laboratories, Inc., Hercules, CA, USA) and image acquisition was performed by Image Lab™ Software (Bio-Rad Laboratories).

Cell migration assays. For the invasion assays, after treatment with different concentrations (0, 2.5, 5 and 10 μmol/l) of OP-B, $5x10^4$ A549 cells in serum-free media were placed into the upper chamber of an insert (8-μm pore size; BD Matrigel Invasion Chamber; BD Biosciences, Franklin Lakes, NJ, USA), and medium containing 10% FBS was added to the lower chamber. After incubation for 24 h, the cells that had migrated through the membrane were fixed with methanol, stained with Giemsa, imaged and counted using a DMI 8 inverted microscope (Leica Microsystems, Wetzlar, Germany).

For the scratch wound healing assay, $3x10^5$ A549 cells in 500 μl of medium were seeded in a culture dish. After 24 h, the confluent cell monolayer was scraped with a pipette tip (10 μl) to generate 4 scratch wounds on each slide and rinsed twice with PBS to remove the floating cells. Then, fresh medium containing 0 (vehicle), 5 or 10 μmol/l OP-B was added; after culture for 6 or 24 h, the images were captured immediately under a phase contrast microscope (DMI 8; Leica Microsystems).

Microtubule formation assay. This experiment was performed in 96-well plates coated with 50 μl of Matrigel (BD Biosciences, Bedford, MA, USA). Then, $1.0x10^4$ EA.hy926 cells were seeded per well. Tubule formation was observed under a phase contrast microscope (DMI 8; Leica Microsystems).

Migration assay in nude mice. The 5-week-old athymic BALB/c mice were maintained under specific pathogen-free (SPF) conditions and manipulated according to protocols approved by the Shanghai Medical Experimental Animal Care Commission. A total of $2x10^7$ A549 cells were injected into the tail vein of nude mice. After 7 days, when the lung metastasis model was successfully generated, the mice were randomly divided into three groups (6 in each group), including the OP-B groups (37.5 or 75 mg/kg p.o. daily; n=6) and the control group (corn oil, 100 μl, p.o. daily; n=6). After 21 days of treatment, the mice were sacrificed by cervical dislocation, and the tissues were isolated for subsequent experiments.

Matrigel plug assay for angiogenesis in nude mice. Athymic male mice were purchased from the Model Animal Research Center of Nanjing University (Nanjing, China) and maintained

Table I. Top canonical pathways in A549 cells.

Name of pathway	P-value	Overlap
Regulation of the epithelial-mesenchymal transition pathway	1.25E-03	9.8% 18/84
Transcriptional regulatory network in embryonic stem cells	1.59E-03	17.5% 7/40
Human embryonic stem cell pluripotency	2.27E-03	10.4% 14/134
Neuropathic pain signaling in dorsal horn neurons	4.36E-03	11.0% 11/100
Estrogen biosynthesis	4.36E-03	15.8% 6/38

under SPF conditions. A549 cells were harvested, washed with phosphate-buffered saline, and resuspended in serum-free medium. Cell aliquots (0.2 ml) were mixed with 0.4 ml of high-concentration Matrigel (BD Biosciences) and immediately injected subcutaneously into the right flank of nude mice. After 7 days, tumor-bearing mice were randomly divided into three groups, including those treated with OP-B (37.5 or 75 mg/kg p.o. daily; n=6) or CMC-Na (control, 100 μl, p.o. daily; n=6) for 14 days. Then, the tumors were isolated for subsequent experiments. The hemoglobin content of the tumor was determined using Drabkin's reagent kit (Sigma-Aldrich; Merck KGaA). All the above experiments in mice were carried out in strict accordance with the Guide for the Care and Use of Laboratory Animals of the National Institutes of Health. Our protocol was approved by the Committee on the Ethics of Animal Experiments of Nanjing University of Chinese Medicine.

Statistical analysis. All the data are expressed as the mean ± SD, and the results were analyzed by Student's t-test. $P<0.05$ indicated statistical significance.

Results

Differentially expressed gene (DGE) library sequencing of 3 NSCLC cell lines treated with OP-B. Six DGE libraries of NSCLC cells were sequenced: A549 (vehicle), A549 (OP-B treatment), NCI-H460 (vehicle), NCI-H460 (OP-B treatment), NCI-H596 (vehicle), and NCI-H596 (OP-B treatment).

After comparing the transcriptomes regulated by OP-B in the 3 cell lines, we found that the sensitivity of different NSCLC cell lines to OP-B differed greatly. In NCI-H460 cells, 530 genes had significantly different expression levels, with 102 and 428 upregulated and downregulated genes, respectively. In A549 or NCI-H596 cells, only 62 or 85 significant differentially expressed genes were detected, with 34 and 32 upregulated and 28 and 53 downregulated genes, respectively. The threshold for judging the statistical significance of gene expression was FDR ≤0.05 and absolute value of log2 ratio ≥1.

Annotation of the molecular pathways altered by OP-B in NSCLC cells. Over-represented Gene Ontology (GO) terms for all DE genes identified in cells treated with OP-B for 24 h were analyzed by Ingenuity pathway analysis, and the canonical pathways of the 3 cell lines regulated by OP-B are shown in Fig. 1. Within these cell lines, we found that the pathways regulated by OP-B were more meaningful in only the A549 cell line, and the top canonical pathway regulated by OP-B was the epithelial-mesenchymal transition (EMT) pathway (Table I).

OP-B regulated EphA2/Akt pathway in the A549 and H460 cell lines. Tight junctions (TJs) between cells promote the binding of EphA2 and Ephrin-A1; then, the endocytosis and degradation of EphA2 occur (16). In contrast, lack of TJs between cells decreases the endocytosis and degradation of EphA2. Crucially, overexpression of EphA2 promoted EMT and cell migration and invasion. From the results, we found that 10 μmol/l OP-B induced the expression of Ephrin-A1 in both A549 and NCI-H460 cells, while the level of EphA2 change differed between them. In A549 cells, OP-B treatment somewhat decreased the expression of EphA2, while in NCI-H460 cells, it significantly increased the level of EphA2, which suggested that TJs might be promoted by OP-B in A549 cells but not in NCI-H460 cells.

Otherwise, activation of EphA2 effectively inhibits the Ras/Erk1/2 and PI3K/Akt pathways (17). The absence of ligand abrogates the autophosphorylation of EphA2 and the subsequent activation of Ras and Akt. Then, EphA2 would be phosphorylated at the cytoplasmic S897 by Akt (18). In our previous study, we reported that OP-B inhibited the PI3K/Akt pathway in several NSCLC cell lines. Here, we found that the phosphorylation of EphA2 (Ser897) was significantly inhibited by OP-B in A549 cells but was stimulated by OP-B in NCI-H460 cells. Meanwhile, in A549 cells, the Raf/ERK pathway was unaffected, while in NCI-H460 cells, the expression of A-Raf and c-Raf was significantly promoted, and the phosphorylation of c-Raf and ERK1/2 was unaffected by OP-B (Fig. 2).

OP-B inhibits the motility and invasiveness of A549 cells in vitro. Specifically, EMT starts by loss of cell junction proteins, including E-cadherin, claudins, occludins and catenins, associated with epithelial organization, followed by expression of the mesenchymal markers N-cadherin and vimentin (19,20). Slug is known to repress the transcription of E-cadherin by binding to its promoter region during development (21). Additionally, binding of Slug to the integrin promoter represses its expression and results in reduced cell adhesion (22). ZEB family proteins are also inhibitors of E-cadherin.

Next, the effects of OP-B on the migration and invasion of A549 cells were investigated, and EMT-related molecules were detected. Using Transwell migration and scratch wound healing assays, we found that OP-B significantly

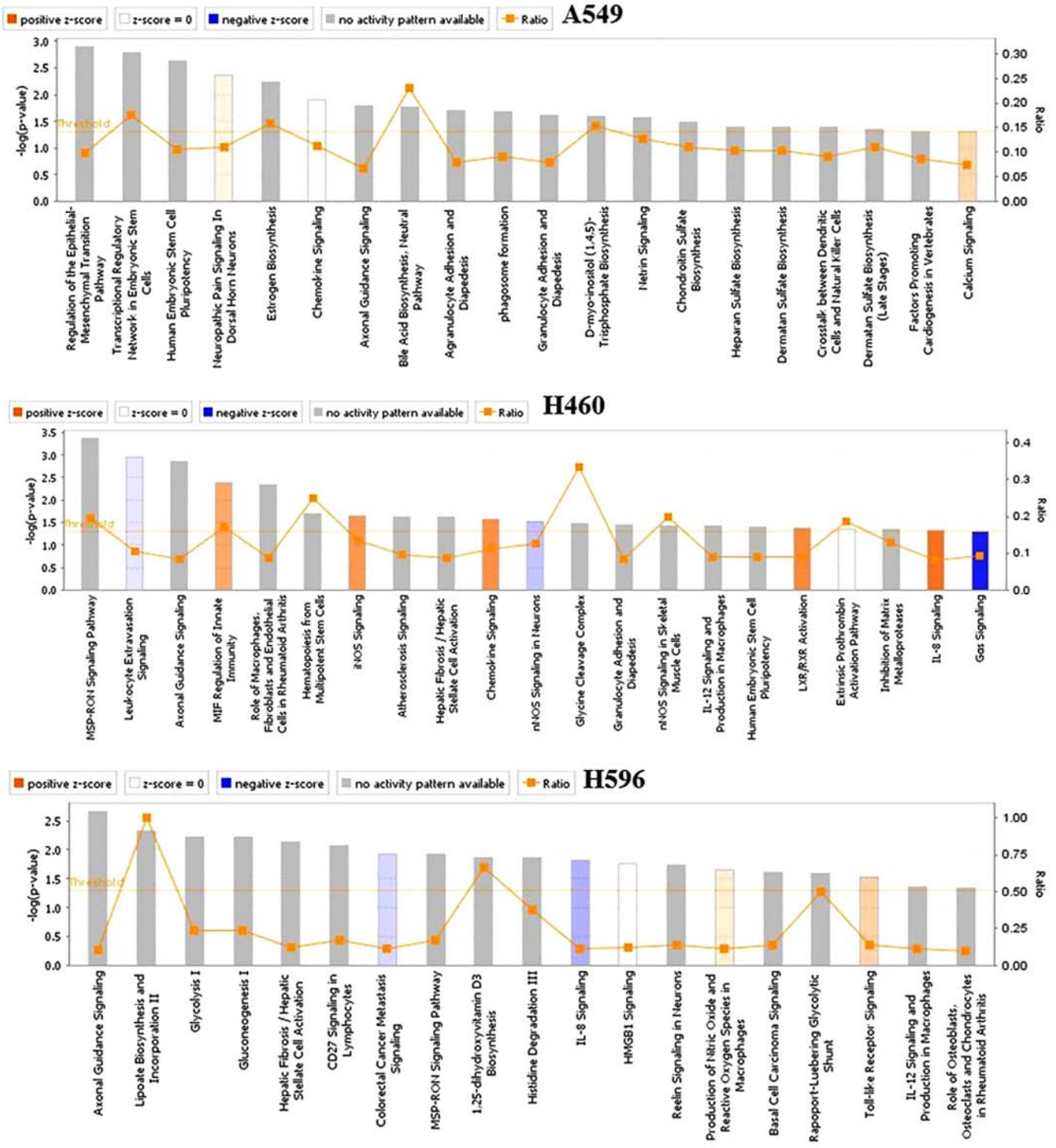

Figure 1. The canonical pathways in the 3 cell lines regulated by OP-B. OP-B, Ophiopogonin B.

reduced the invasion ability (Fig. 3A and B) and inhibited the wound closure of A549 cells at a concentration of 10 μmol/l (Fig. 3C).

Detection of EMT-associated proteins showed that besides vimentin, which was unaffected by OP-B, N-cadherin, Snail, Slug and TCF8/ZEB1 were all inhibited by 10 μmol/l OP-B, and E-cadherin and ZO-1 were upregulated by OP-B (Fig. 3D).

In addition, Src is known to integrate and regulate RTK signaling and to transduce survival signals to PI3K/Akt and STAT3 (23). Src activation dissociates cell junctions and facilities cell mobility. Src activation also stabilizes focal adhesion complexes through FAK phosphorylation (11).

Detection of this Src-associated pathway showed that 10 μmol/l OP-B inhibited the phosphorylation of Src, FAK, Stat3 and Stat5 at the same time (Fig. 3E).

More importantly, 75 mg/kg OP-B significantly reduced the number of metastatic nodules compared with the control treatment group and this difference was further confirmed by examination of hematoxylin and eosin (H&E)-stained lung sections (Fig. 3F).

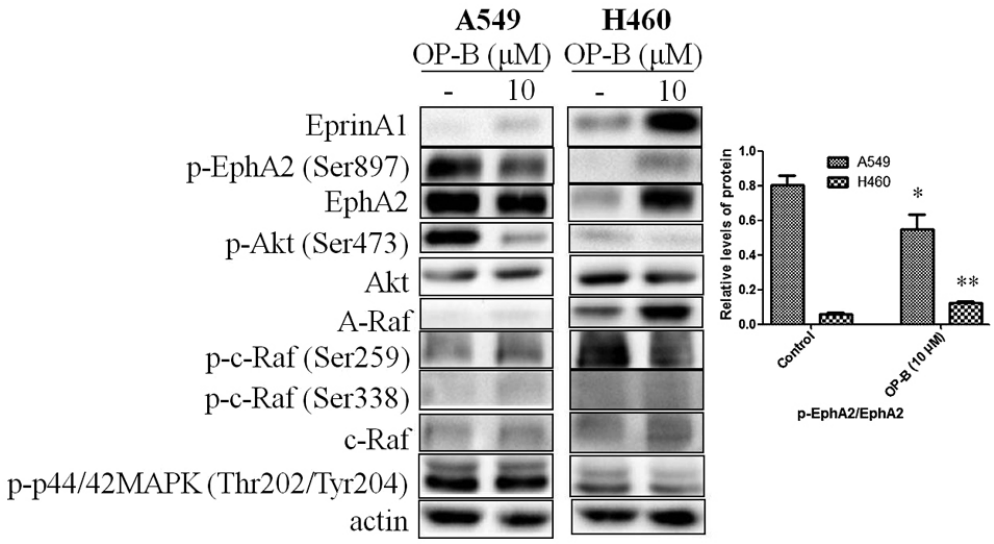

Figure 2. Effects of OP-B on EphA2/Akt signaling pathway in A549 and NCI-H460 cells. A549 or NCI-H460 cells were treated with or without 10 μmol/l OP-B for 24 h, and then, the expression levels of EphrinA1, EphA2, A-Raf, and c-Raf and the phosphorylation levels of Akt (Ser473), EphA2 (Ser897), c-Raf (Ser259), c-Raf (Ser338), and ERK1/2 were detected by western blotting. β-actin was used as a loading control. The experiment was repeated three times and yielded similar results. Densitometric analysis of the western blots (right); n=3. *P<0.05 and **P<0.01 represent significant differences compared with control cells. OP-B, Ophiopogonin B.

OP-B inhibits angiogenesis in vitro and in vivo. To determine the anti-angiogenesis effect of OP-B on endothelial cells, we performed a tubule formation assay in EA.hy926 cells. As shown in Fig. 4A, 5 μmol/l OP-B obviously promoted tube formation from 2 to 4 h, while 10 μmol/l OP-B obviously inhibited tube formation in EA.hy926 cells. Detection of angiogenesis-regulating proteins showed that OP-B significantly inhibited the expression of VEGFR2 and Tie-2 at a concentration of 10 μmol/l (Fig. 4B). Meanwhile, phosphorylation of the downstream proteins Akt (S473) and PLC (S1248) was also inhibited by OP-B. In addition, the levels of EphA2 and phosphorylated EphA2 (S897) were also inhibited by OP-B (Fig. 4C).

In vivo, we used a Matrigel plug assay to determine the anti-angiogenesis effects of OP-B in nude mice. After intragastric administration of 37.5 or 75 mg/kg OP-B on 14 consecutive days, the tumors were isolated and photographed, and the hemoglobin content of the Matrigel plug was determined using Drabkin's reagent kit according to the manufacturer's instructions. As shown in Fig. 5A and B, tumor angiogenesis was obviously inhibited by OP-B, and hemoglobin content was significantly inhibited by OP-B (Fig. 5C).

Discussion

Local invasion and tumor metastasis occur with high incidence in the clinic. Alterations in cell-cell and cell-matrix adhesion molecules are associated with the progression of tumor malignancy.

Whole transcriptome analyses are widely used to characterize the underlying mechanisms based on global gene expression changes in different cancers (24). Genomic information on Ophiopogonin B (OP-B) in different NSCLC cell lines is currently unavailable, and transcriptome and expression profiling data for OP-B-regulated genes in different NSCLC cell lines are needed as an important resource to better understand the regulatory mechanisms of OP-B in NSCLC cell lines.

Histologically, lung adenocarcinoma is the most common metastatic cancer, which is responsible for its high patient mortality. Thus, the investigation of anti-metastatic agents for lung adenocarcinoma is crucial for lung cancer treatment. In this investigation, the obtained NSCLC cell line transcriptome and DGE profiling data provide comprehensive information on gene expression regulated by OP-B in different NSCLC cell lines, which facilitates our understanding of the molecular mechanisms mediated by OP-B in these cell lines and provides new insight into the regulation of EMT and metastasis in A549 cells by OP-B.

To verify the results of the former transcriptome analysis and to verify the role of the EphA2/Akt pathway in OP-B-regulated EMT, we chose the A549 and NCI-H460 cell lines for further experiments. From the results, we found that 10 μmol/l OP-B promoted the expression of Ephrin-A1 in both A549 and NCI-H460 cells, while the level of EphA2 was altered differentially in these two cell lines. In A549 cells, OP-B treatment decreased the expression of EphA2, while in NCI-H460 cells, it significantly increased the level of EphA2, which suggested that OP-B promoted tight junctions (TJs) in A549 cells but not in NCI-H460 cells. In addition, with the lack of ligand binding, the auto-tyrosine phosphorylation of EphA2 and subsequent suppression of Ras and Akt are abrogated; then, activated Akt can phosphorylate EphA2 at the cytoplasmic S897 (17). Thus, elevated levels of phosphorylated EphA2 (S897) predict the increased ability for cell mobility. Here, we found that the phosphorylation of EphA2 (Ser897) was significantly inhibited by OP-B in A549 cells but stimulated by OP-B in NCI-H460 cells. The Ras/ERK pathway was unaffected in A549 cells and enhanced in NCI-H460 cells by OP-B (Fig. 2). Therefore, the results indicated that OP-B may inhibit invasion and mobility in A549 cells. In fact, through

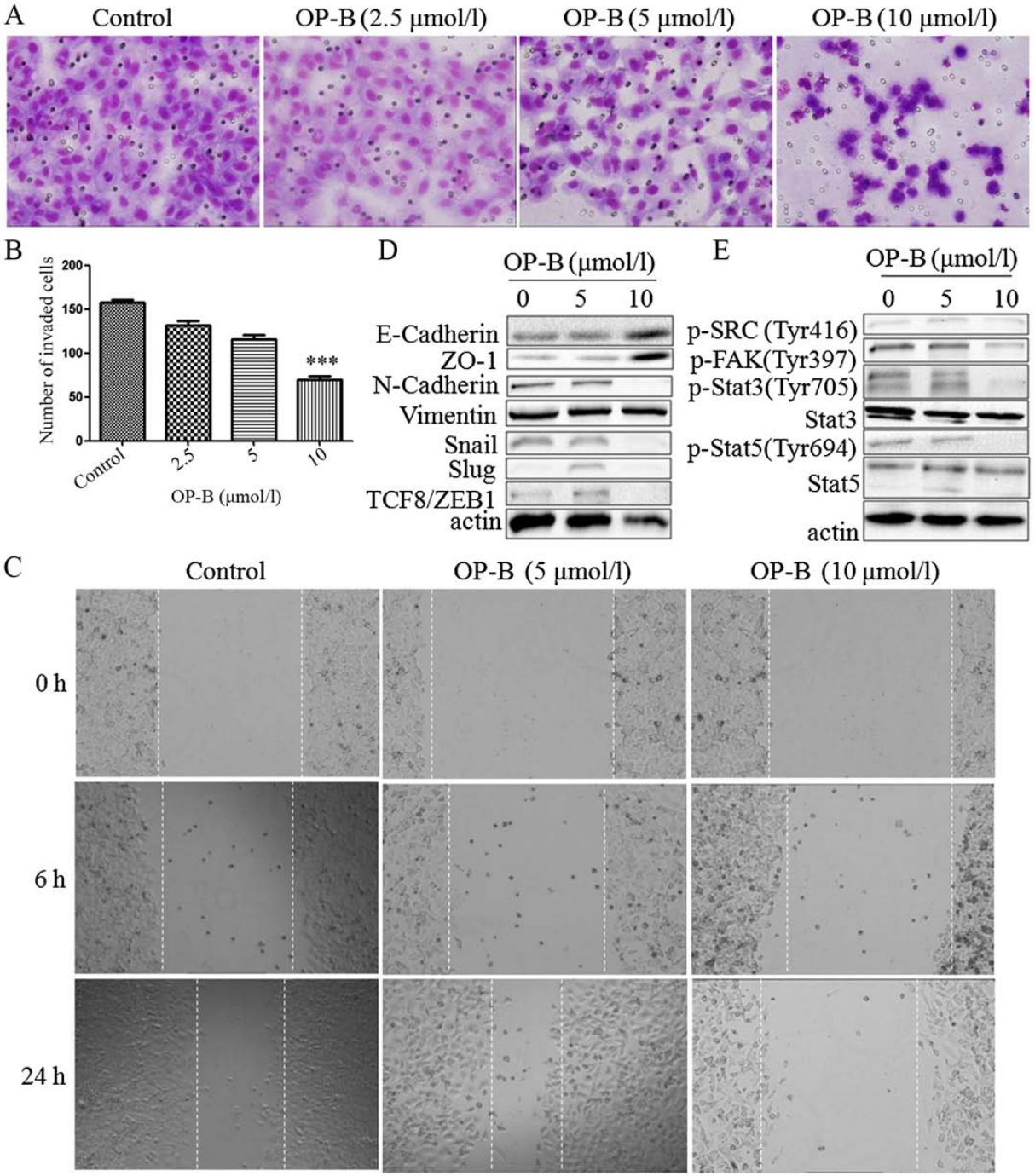

Figure 3. OP-B inhibits the invasion and migration of A549 cells *in vitro* and *in vivo*. (A) Transwell migration and invasion assays were performed to examine cell migration and invasion in A549 cells. Representative images of migrated or invaded cells are displayed (magnification, x200). (B) Columns indicate the mean ± SD of triplicate experiments (***P<0.001, independent Student's t-test). (C) Wound healing assays were used to investigate the motility of A549 cells treated with OP-B, and representative images are shown (magnification, x40). (D and E) A549 cells were treated with or without 10 μmol/l OP-B for 24 h, and then, the expression levels of vimentin, N-cadherin, E-cadherin, ZO-1, Snail, Slug, TCF8/ZEB1, p-SRC (Tyr416), p-FAK (Tyr397), p-Stat3 (Tyr705), Stat3, p-Stat5 (Tyr694) and Stat5 were detected by western blotting. β-actin was used as a loading control. The experiment was repeated three times and yielded similar results. OP-B, Ophiopogonin B.

the Transwell migration and scratch wound healing assays, we found that 10 μmol/l OP-B significantly reduced the invasion and migration ability of A549 cells *in vitro* (Fig. 3A-C). *In vivo*, we also found that 75 mg/kg OP-B i.g. inhibited A549 cell metastasis in the lung metastasis nude mouse model. Detection of the protein showed that the mechanism correlated with the inhibition of EphA2. Further detection of EMT-related molecules showed that OP-B treatment increased expression of the epithelial markers ZO-1 and E-cadherin but decreased the expression of the mesenchymal marker N-cadherin and the transcriptional repressors Snail, Slug and ZEB1. In addition, the impact of OP-B on EMT also correlated with inhibition of the activation of the non-receptor tyrosine kinase Src and its downstream pathway.

In addition to EMT, tumor neoangiogenesis is also involved in the development of metastasis from a primary tumor site and

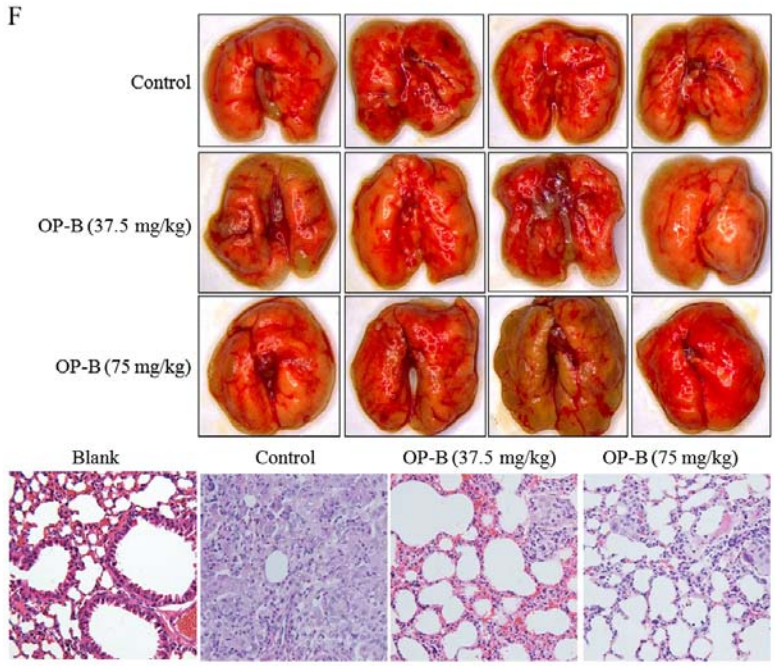

Figure 3. Continued. OP-B inhibits the invasion and migration of A549 cells *in vitro* and *in vivo*. (F) OP-B inhibits the lung metastasis of A549 cells *in vivo*. Representative images of H&E-stained metastatic lung nodules. OP-B, Ophiopogonin B.

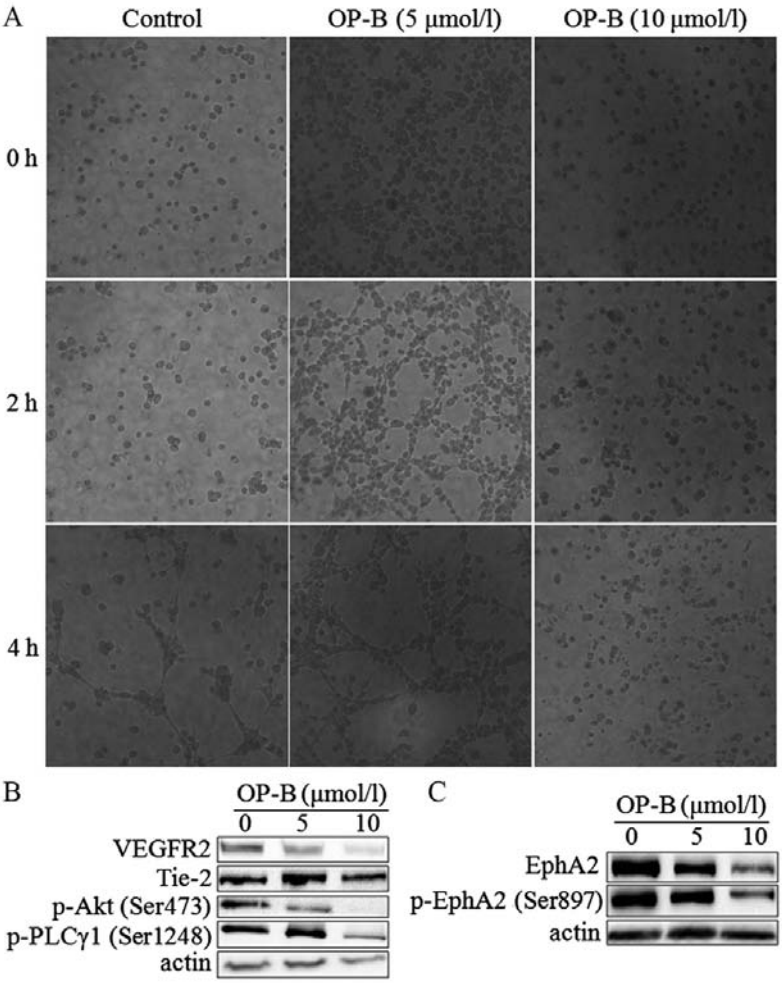

Figure 4. OP-B inhibits tubule formation by endothelial cells. (A) Matrigel assay analysis was used to detect microtubule formation by EA.hy926 cells after treatment with 0, 5, or 10 μmol/l OP-B for 0, 2, or 4 h. Representative images are displayed (magnification, x200). (B and C) A549 cells were treated with 0, 5 or 10 μmol/l OP-B for 24 h, and the phosphorylation levels of VEGFR2, Tie-2, p-Akt (Ser473), p-PLCγ1 (Ser1248), EphA2, and p-EphA2 (Ser897) were detected by western blotting. β-actin was used as a loading control. The experiment was repeated three times and yielded similar results. OP-B, Ophiopogonin B.

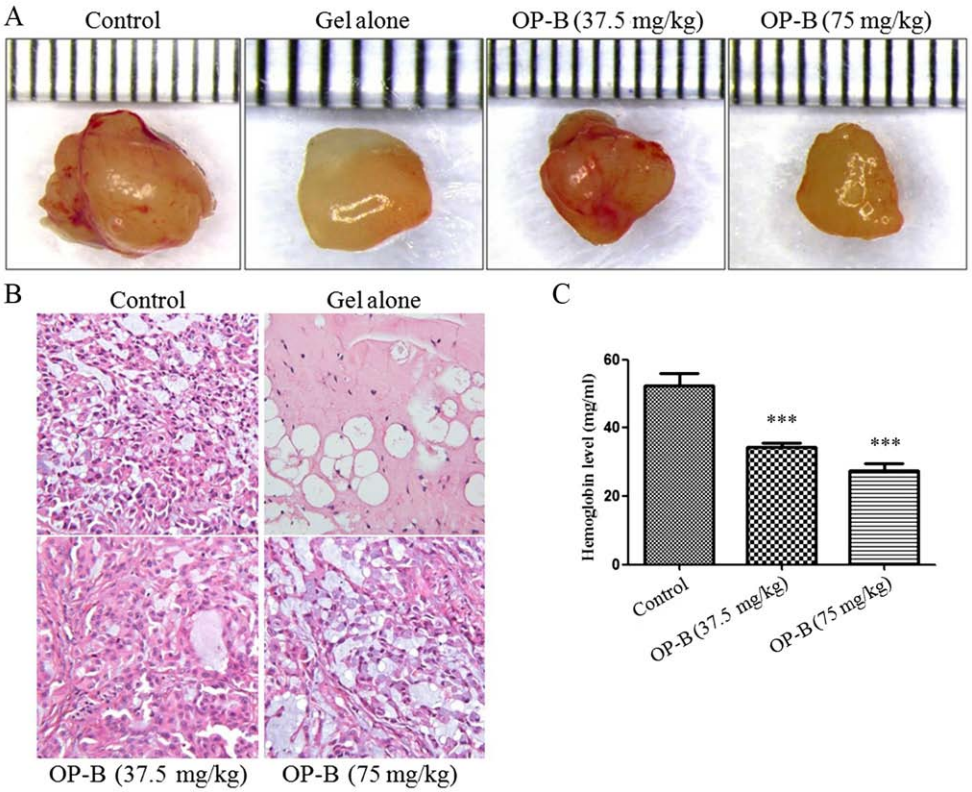

Figure 5. OP-B inhibits angiogenesis *in vivo*. (A and B) Tumor angiogenesis was significantly inhibited by 37.5 or 75 mg/kg OP-B. (C) The hemoglobin content of the Matrigel plugs was determined using Drabkin's reagent kit. The results are expressed as the mean ± SD (n=5) (Error bars, SD; $^{***}P<0.001$). OP-B, Ophiopogonin B.

spread of malignancy. *In vitro*, we found that 10 μmol/l OP-B obviously inhibited tube formation in EA.hy926 cells (Fig. 4A). Detection of angiogenesis-regulating proteins showed that OP-B obviously inhibited the expression of VEGFR2 and Tie-2 at a concentration of 10 μmol/l and downregulated the phosphorylation of Akt (S473) and PLC (S1248). More importantly, the levels of EphA2 and phosphorylated EphA2 (S897) were also inhibited by OP-B (Fig. 4B and C). *In vivo*, through the Matrigel plug assay, we found that tumor angiogenesis was inhibited by OP-B (Fig. 5A and B); meanwhile, hemoglobin content was significantly inhibited by OP-B (Fig. 5C).

Taken together, through improving TJs junctions between A549 cells, OP-B inhibited EMT and then regulated the EphA2/Akt/Raf/ERK and Src/FAK/Stat pathways in the cells. By these mechanisms, OP-B inhibited the metastasis of A549 cells *in vitro* and *in vivo*. Meanwhile, through inhibiting the VEGFR2/Tie2/Akt/PLC and EphA2 pathways, OP-B also inhibited angiogenesis of A549 tumors *in vivo* (Fig. 6).

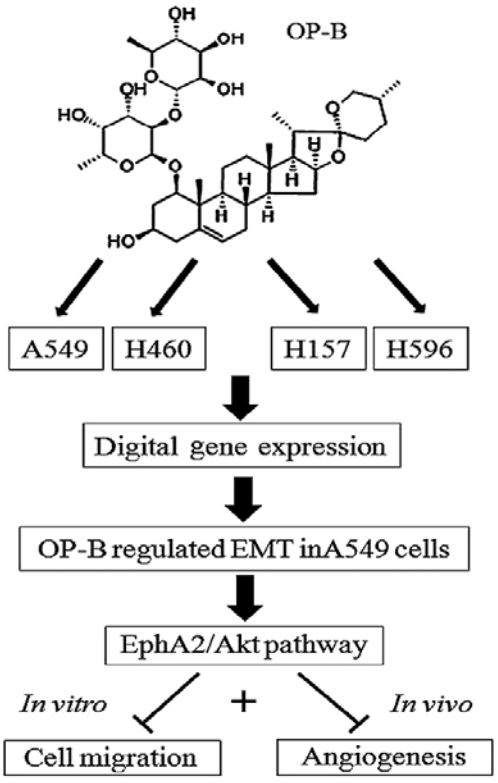

Figure 6. The proposed mechanism of OP-B in A549 cells. Ingenuity pathway analysis of the digital gene expression indicates that OP-B specifically regulates the epithelial-mesenchymal transition pathway in A549 adenocarcinoma cells. Through inhibiting the EphA2/Akt/Raf/ERK and Src/FAK/Stat pathways in the cells, OP-B inhibits the metastasis and angiogenesis of A549 cells *in vitro* and *in vivo*. OP-B, Ophiopogonin B.

Acknowledgements

The authors thank Professor Zhigang Tu (Jiangsu University, China) for providing the EA.hy926 cell line.

Funding

The present study was supported by the National Natural Science Foundation of China (grant no. 81503374), the Priority Academic Program Development of Jiangsu Higher Education Institutions (PAPD), the Natural Science Foundation of

Jiangsu Province (grant no. BK20151003) and the Research Foundation of Education Bureau of Jiangsu Province (grant no. 16KJA360001).

Availability of data and materials

The datasets used during the present study are available from the corresponding author upon reasonable request.

Authors' contributions

XZ, HF and MW conceived and designed the study. MC, CH, RJ, YG, HJ and YZ performed the experiments. MC wrote the manuscript. All authors read and approved the manuscript and agree to be accountable for all aspects of the research in ensuring that the accuracy or integrity of any part of the work are appropriately investigated and resolved.

Ethics approval and consent to participate

All the above experiments in mice were carried out in strict accordance with the Guide for the Care and Use of Laboratory Animals of the National Institutes of Health. Our protocol was approved by the Committee on the Ethics of Animal Experiments of Nanjing University of Chinese Medicine.

Patient consent for publication

Not applicable.

Competing interests

The authors declare that they have no competing interests.

References

1. Collins LG, Haines C, Perkel R and Enck RE: Lung cancer: Diagnosis and management. Am Fam Physician 75: 56-63, 2007.
2. Riihimaki M, Hemminki A, Fallah M, Thomsen H, Sundquist K, Sundquist J and Hemminki K: Metastatic sites and survival in lung cancer. Lung Cancer 86: 78-84, 2014.
3. De Craene B and Berx G: Regulatory networks defining EMT during cancer initiation and progression. Nat Rev Cancer 13: 97-110, 2013.
4. Yang G, Liang Y, Zheng T, Song R, Wang J, Shi H, Sun B, Xie C, Li Y, Han J, *et al*: FCN2 inhibits epithelial-mesenchymal transition-induced metastasis of hepatocellular carcinoma via TGF-β/Smad signaling. Cancer Lett 378: 80-86, 2016.
5. Tandon M, Vemula SV and Mittal SK: Emerging strategies for EphA2 receptor targeting for cancer therapeutics. Expert Opin Ther Targets 15: 31-51, 2011.
6. Huang J, Xiao D, Li G, Ma J, Chen P, Yuan W, Hou F, Ge J, Zhong M, Tang Y, *et al*: EphA2 promotes epithelial-mesenchymal transition through the Wnt/β-catenin pathway in gastric cancer cells. Oncogene 33: 2737-2747, 2014.
7. Udayakumar D, Zhang G, Ji Z, Njauw CN, Mroz P and Tsao H: EphA2 is a critical oncogene in melanoma. Oncogene 30: 4921-4929, 2011.
8. Dunne PD, Dasgupta S, Blayney JK, McArt DG, Redmond KL, Weir JA, Bradley CA, Sasazuki T, Shirasawa S, Wang T, *et al*: EphA2 expression is a key driver of migration and invasion and a poor prognostic marker in colorectal cancer. Clin Cancer Res 22: 230-242, 2016.
9. Wang W, Lin P, Sun B, Zhang S, Cai W, Han C, Li L, Lu H and Zhao X: Epithelial-mesenchymal transition regulated by EphA2 contributes to vasculogenic mimicry formation of head and neck squamous cell carcinoma. Biomed Res Int 2014: 803914, 2014.
10. Song W, Ma Y, Wang J, Brantley-Sieders D and Chen J: JNK signaling mediates EPHA2-dependent tumor cell proliferation, motility, and cancer stem cell-like properties in non-small cell lung cancer. Cancer Res 74: 2444-2454, 2014.
11. Parri M, Buricchi F, Giannoni E, Grimaldi G, Mello T, Raugei G, Ramponi G and Chiarugi P: EphrinA1 activates a Src/focal adhesion kinase-mediated motility response leading to rho-dependent actino/myosin contractility. J Biol Chem 282: 19619-19628, 2007.
12. Zhang S and Yu D: Targeting Src family kinases in anti-cancer therapies: Turning promise into triumph. Trends Pharmacol Sci 33: 122-128, 2012.
13. Chen M, Du Y, Qui M, Wang M, Chen K, Huang Z, Jiang M, Xiong F, Chen J, Zhou J, *et al*: Ophiopogonin B-induced autophagy in non-small cell lung cancer cells via inhibition of the PI3K/Akt signaling pathway. Oncol Rep 29: 430-436, 2013.
14. Chen M, Guo Y, Zhao R, Wang X, Jiang M, Fu H and Zhang X: Ophiopogonin B induces apoptosis, mitotic catastrophe and autophagy in A549 cells. Int J Oncol 49: 316-324, 2016.
15. Naudin C, Sirvent A, Leroy C, Larive R, Simon V, Pannequin J, Bourgaux JF, Pierre J, Robert B, Hollande F and Roche S: SLAP displays tumour suppressor functions in colorectal cancer via destabilization of the SRC substrate EPHA2. Nat Commun 5: 3159, 2014.
16. Wykosky J, Palma E, Gibo DM, Ringler S, Turner CP and Debinski W: Soluble monomeric EphrinA1 is released from tumor cells and is a functional ligand for the EphA2 receptor. Oncogene 27: 7260-7273, 2008.
17. Yang NY, Fernandez C, Richter M, Xiao Z, Valencia F, Tice DA and Pasquale EB: Crosstalk of the EphA2 receptor with a serine/threonine phosphatase suppresses the Akt-mTORC1 pathway in cancer cells. Cell Signal 23: 201-212, 2011.
18. Miao H, Li DQ, Mukherjee A, Guo H, Petty A, Cutter J, Basilion JP, Sedor J, Wu J, Danielpour D, *et al*: EphA2 mediates ligand-dependent inhibition and ligand-independent promotion of cell migration and invasion via a reciprocal regulatory loop with Akt. Cancer Cell 16: 9-20, 2009.
19. Garg M: Epithelial-mesenchymal transition-activating transcription factors-multifunctional regulators in cancer. World J Stem Cells 5: 188-195, 2013.
20. Alizadeh AM, Shiri S and Farsinejad S: Metastasis review: From bench to bedside. Tumour Biol 35: 8483-8523, 2014.
21. Bolos V, Peinado H, Pérez-Moreno MA, Fraga MF, Esteller M and Cano A: The transcription factor Slug represses E-cadherin expression and induces epithelial to mesenchymal transitions: A comparison with Snail and E47 repressors. J Cell Sci 116: 499-511, 2003.
22. Turner FE, Broad S, Khanim FL, Jeanes A, Talma S, Hughes S, Tselepis C and Hotchin NA: Slug regulates integrin expression and cell proliferation in human epidermal keratinocytes. J Biol Chem 281: 21321-21331, 2006.
23. Playford MP and Schaller MD: The interplay between Src and integrins in normal and tumor biology. Oncogene 23: 7928-7946, 2004.
24. Barrett CL, DeBoever C, Jepsen K, Saenz CC, Carson DA and Frazer KA: Systematic transcriptome analysis reveals tumor-specific isoforms for ovarian cancer diagnosis and therapy. Proc Natl Acad Sci USA 112: E3050-E3057, 2015.